JACS
JOURNAL OF THE AMERICAN CHEMICAL SOCIETY
Communication
pubs.acs.org/JACS

Rate-Determining Water-Assisted O−O Bond Cleavage of an Fe^{III}-OOH Intermediate in a Bio-inspired Nonheme Iron-Catalyzed Oxidation

Williamson N. Oloo, Andrew J. Fielding, and Lawrence Que, Jr.*

Department of Chemistry and Center for Metals in Biocatalysis, University of Minnesota, Minneapolis, Minnesota 55455, United States

Supporting Information

ABSTRACT: Hydrocarbon oxidations by bio-inspired nonheme iron catalysts and H_2O_2 have been proposed to involve an Fe^{III}-OOH intermediate that decays via a water-assisted mechanism to form an $Fe^{V}(O)(OH)$ oxidant. Herein we report kinetic evidence for this pathway in the oxidation of 1-octene catalyzed by $[Fe^{II}(TPA)(NCCH_3)]^{2+}$ (**1**, TPA = tris(2-pyridylmethyl)-amine). The $(TPA)Fe^{III}(OOH)$ intermediate **2** can be observed at −40 °C and is found to undergo first-order decay, which is accelerated by water. Interestingly, the decay rate of **2** is comparable to that of product formation, indicating that the decay of **2** results in olefin oxidation. Furthermore, the Eyring activation parameters for the decay of **2** and product formation are identical, and both processes are associated with an H_2O/D_2O KIE of 2.5. Taken together with previous ^{18}O-labeling data, these results point to a water-assisted heterolytic O−O bond cleavage of **2** as the rate-limiting step in olefin oxidation.

The development of efficient, selective, and atom-economical methods for the oxidative functionalization of hydrocarbons remains a significant challenge in synthetic organic chemistry.[1] Inspired by the nonheme iron enzymes Nature has evolved to activate dioxygen and carry out hydrocarbon oxidations,[2] we and others have identified nonheme iron complexes of tetradentate N4 ligands that catalyze alkane and alkene oxidations using H_2O_2 as oxidant.[3] These efforts have led to the first examples of iron-catalyzed *cis*-dihydroxylation of olefins[4] and naphthalene,[5] as well as the development of chiral catalysts for enantioselective olefin epoxidation[6] and *cis*-dihydroxylation[7] and for the hydroxylation of aliphatic secondary and tertiary C−H bonds in complex organic molecules with predictable regio- and stereoselectivity.[8] The high stereoretention observed in these transformations and the predictable selectivity demonstrated for C−H bond functionalization strongly argue against the involvement of $HO^{\bullet}$ radicals and implicate a more selective metal-based oxidant.

Early work by Que and co-workers focusing on the catalyst $[Fe^{II}(TPA)(NCCH_3)_2]^{2+}$ (**1**, TPA = tris(2-pyridylmethyl)-amine) led to the low-temperature trapping and spectroscopic characterization of a low-spin Fe^{III}-OOH intermediate **2**.[9] This species was excluded as the actual oxidant on the basis of isotopic labeling experiments that showed label incorporation from $H_2{}^{18}O$ into the alkane and alkene oxidation products.[4b,9a] Instead, the Fe^{III}-OOH complex was proposed to undergo water-assisted O−O bond heterolysis to generate an $Fe^{V}(O)(OH)$ species, a notion supported by DFT calculations that found an energetically feasible barrier for this transformation.[10] Evidence for this unprecedented high-valent species has recently been obtained by Costas and Cronin from variable-temperature mass spectrometric analysis of the reaction mixture of a related Fe(N4) catalyst.[11] The O−O bond cleavage step was proposed to be facilitated by the binding of water at the sixth site of the Fe^{III}-OOH complex (Scheme 1), resulting in a hydrogen-bonding interaction between the bound water and the distal oxygen atom of the coordinated hydroperoxide to form a five-membered ring that promotes the loss of the terminal OH functionality as water. This step also generates an $Fe^{V}(O)(OH)$ oxidant that possesses an oxo atom from H_2O_2 and a hydroxo atom from water, where transfer of both O atoms to an olefin substrate affords a mixed-labeled *cis*-diol product as observed. On the other hand, the epoxide product shows only partial label incorporation from $H_2{}^{18}O$ due to oxo−hydroxo tautomerism prior to the O-atom transfer step. Given the progress in this field within the past decade, we have returned to the original observations and report herein the first kinetic evidence that supports the water-assisted mechanism presented in Scheme 1.

Scheme 1. Proposed Mechanism of Olefin Oxidation by a Nonheme Iron Catalyst and H_2O_2 in CH_3CN That Accounts for the Observed Pattern of O-Atom Incorporation into Products from H_2O_2 and Water

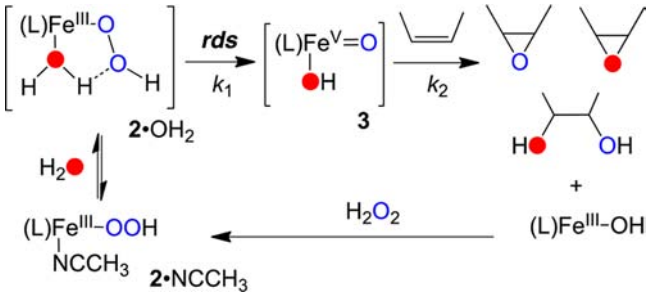

Received: March 18, 2013
Published: April 17, 2013

   dx.doi.org/10.1021/ja402759c | *J. Am. Chem. Soc.* 2013, 135, 6438−6441

Our kinetic studies of the catalytic oxidation of 1-octene by **1** and H_2O_2 were carried out at −40 °C by monitoring the reaction mixture as a function of time via UV−visible spectroscopy and GC analysis of reaction products from aliquots that were quenched at this low temperature (Figure 1).[12] As shown in Figure 1, the addition of 20 equiv of H_2O_2

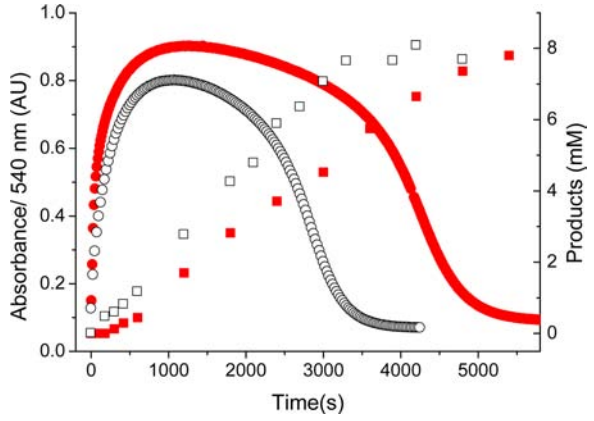

Figure 1. Time course for the oxidation of 1-octene (250 equiv) by 1.0 mM **1** and 20 equiv of H_2O_2 in CH_3CN at −40 °C as monitored by the appearance and decay of **2** at 540 nm (circles) and by the formation of olefin oxidation products determined by GC (squares). The reactions were conducted in the presence of 80 (red) or 116 (black) equiv of H_2O.

(30%) to a 1.0 mM solution of **1** in MeCN at −40 °C in the presence of 0.25 M 1-octene resulted in the rapid formation of a chromophore at 540 nm in ∼90% yield that is associated with $[(TPA)Fe^{III}(OOH)(solvent)]^{2+}$ (**2**).[4b,9,13] This species is the best spectroscopically characterized Fe^{III}-OOH intermediate thus far from this family of nonheme iron catalysts. Following formation of **2**, a pseudo-steady-state phase was observed from ∼700 to ∼3500 s (Figure 1), after which the concentration of **2** dropped precipitously. The appearance of a steady-state phase strongly suggests that the rate of decay of **2** is comparable to that of its re-formation so long as excess H_2O_2 is present. The abrupt decrease of **2** in the last phase can then be ascribed to the depletion of the H_2O_2 and is readily fit with a single exponential function, indicating a first-order decay process with k_{decay} = 0.0024(3) s^{-1}. This decay rate was found to be independent of the amount of 1-octene present (Table S1). Related nonheme low-spin Fe^{III}-OOH intermediates involved in benzene hydroxylation investigated by Rybak-Akimova[14] and Banse[15] have also been observed to undergo exponential decay at rates that were unaffected by the concentration of benzene. These kinetic observations suggest that low-spin Fe^{III}-OOH intermediates are not directly involved in substrate oxidation.

Despite the substrate-independent decay noted above, 1-octene oxidation products were observed to form at −40 °C over the same time period as the formation and decay of **2** (Figure 1). Interestingly, there was an initial lag phase of ∼300 s before any olefin oxidation products were observed, which corresponded to the accumulation of ∼75% of **2**. After the lag phase, both epoxide and diol products were observed to form linearly with time over the next 4000 s. Product formation then ceased when **2** had decayed completely, indicating that **2** is required for olefin oxidation. The slope of the linear phase of product formation essentially represents a catalytic olefin oxidation rate (V_o) of 0.0018(2) mM/s for the combined amount of epoxide and diol products. The corresponding unimolecular rate constant (k_{cat}) of 0.0018(2) s^{-1}, which is obtained by dividing the olefin oxidation product formation rate V_o by the catalyst concentration (1.0 mM), compares well with the decay rate of **2** (0.0024(3) s^{-1}). Taken together, the above results demonstrate that olefin oxidation can occur at −40 °C with **1** as catalyst, and that the decay of **2** is the rate-determining step. Thus, despite the perceived "sluggishness" of an Fe^{III}-OOH species as an oxidant,[16] these results demonstrate that intermediate **2** is definitely involved in olefin oxidation.

As suggested earlier by the ^{18}O-labeling experiments, **2** is not the oxidant itself but rather the precursor to the actual oxidant that must incorporate an O atom from water.[4b] A likely mechanism for $H_2{}^{18}O$-label incorporation is the ligand exchange of water into **2**·$NCCH_3$, forming **2**·OH_2[17] (Scheme 1). In support of this mechanistic hypothesis, we found that the rates of both **2** decay and product formation were sensitive to the amount of water present in the solution. As shown in Figure 1, increasing the water concentration shortened the steady-state phase and enhanced the rates of **2** decay and product formation. A more systematic study of the water effect in Figure 2 demonstrated the accelerative effect of water on the

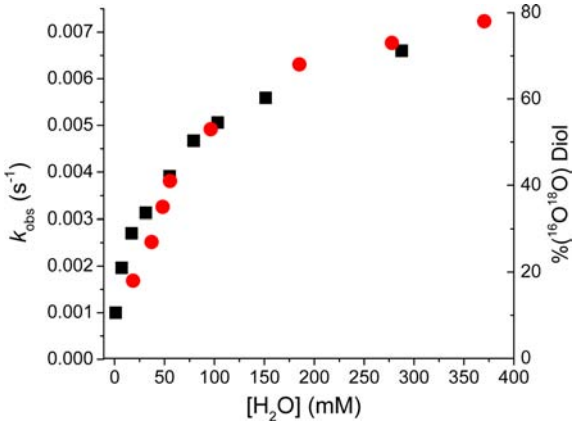

Figure 2. Water concentration dependence for the decay rate of **2** (prepared from the reaction of **1** in CH_3CN with 10 equiv of 70% H_2O_2) at −40 °C (black squares) and the fraction of *cis*-diol with a single ^{18}O-label obtained in the oxidation of 1-octene by **1** and H_2O_2 in the presence of $H_2{}^{18}O$ at 0 °C (red circles).

rate of decay of **2** until it plateaued above 0.3 M. This observed saturation behavior indicates the presence of a rapidly established pre-equilibrium binding of H_2O onto the iron center that precedes the decay of the water adduct. Fitting the water dependence with a one-site ligand binding function[18] gives an apparent association constant of 30 M^{-1} (Figure S3). This value is in reasonable agreement with the value of 12 M^{-1} for the extent of $H_2{}^{18}O$ incorporation into the octane-1,2-diol from **1**-catalyzed 1-octene oxidation at 0 °C (Figure S4) and the value of 16 M^{-1} reported by Chen and Que for the extent of $H_2{}^{18}O$ labeling of the cyclohexanol derived from **1**-catalyzed cyclohexane hydroxylation at 25 °C.[9a] The similarity in the equilibrium constants between the isotope labeling experiments and the decay rate of **2** as a function of water concentration indicates that reversible binding of water onto the iron center of intermediate **2** is involved in its decay and in isotope label incorporation into the oxidation products (Scheme 1). The replacement of the CH_3CN solvent ligand with water in **2** thus accelerates O−O bond cleavage.

dx.doi.org/10.1021/ja402759c | *J. Am. Chem. Soc.* 2013, 135, 6438−6441

Strong corroboration of this notion derives from comparing results in the presence of 100 equiv of added H_2O or D_2O (Figure 3). Note the effect of D_2O in lengthening the steady-state phase and decreasing the rates of **2** decay and formation of oxidation products. Indeed, a kinetic isotope effect (KIE) of 2.5 was observed for the decay of **2** (Figure 3 top) and for the corresponding rate of product formation (Figure 3 bottom). These results demonstrate the important role for a proton in the rate-determining cleavage of the O−O bond. For comparison, similar KIE values have been observed for other O−O bond cleavage steps that lead to the formation of high-valent intermediates, such as the conversion of Cpd O to Cpd I by horseradish peroxidase (1.7),[19] the formation of a model Cpd I from the reaction of a peracid with a synthetic iron(III) porphyrin complex (2),[20] and the conversion of the diiron(III)−peroxo intermediate of soluble methane monooxygenase to the diiron(IV) intermediate **Q** (1.4 and 1.8).[21] Taken together, these data provide for the first time direct kinetic evidence that the decay of the Fe^{III}-OOH species **2** corresponds to the rate-limiting step in the olefin oxidation reaction. The fact that a proton facilitates O−O bond cleavage strongly implicates an O−O bond heterolysis mechanism where protonation mitigates the incipient negative charge formed on the leaving O atom.

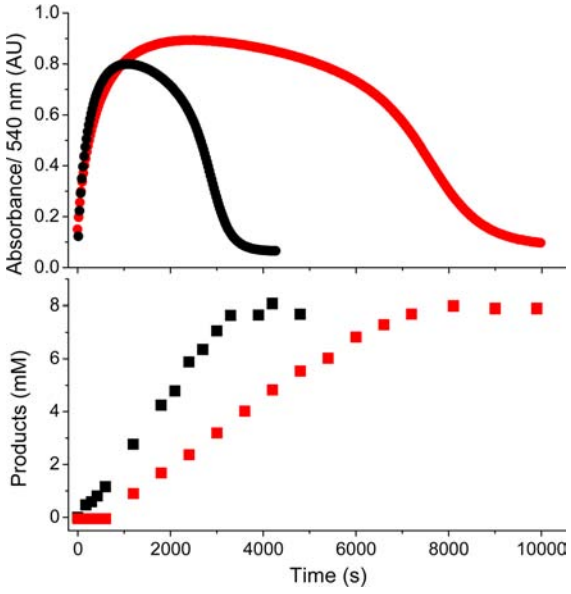

Figure 3. Time courses for the formation and decay of **2** as monitored via UV−vis spectroscopy in the oxidation of 1-octene (250 equiv) by 1.0 mM **1** and 20 equiv of 70% H_2O_2 in CH_3CN at −40 °C (top) and for the combined amounts of 1,2-octanediol and 1,2-epoxyoctane formed under the same reaction conditions as monitored via GC (bottom) in the presence of 100 equiv of H_2O (black shapes) or D_2O (red shapes).

An Eyring analysis of the temperature dependence of the decay rate of **2** in the presence of 1-octene (250 equiv) afforded activation parameters of 45(2) kJ/mol for enthalpy and −95(10) J/K·mol for entropy (Figure 4). The corresponding k_{cat} values for 1-octene oxidation have also been determined at several temperatures and found to fall on the Eyring plot (within error) shown in Figure 4. Together, these data strongly support our conclusion that the rate-determining step in olefin oxidation corresponds to the decay of **2**. The Eyring parameters obtained for **2** can be compared to values reported for other nonheme iron−peroxo complexes (Table 1).[9b,22] Scrutiny of these values shows that the activation enthalpy for the decay of **2** is about 10 kJ/mol smaller than those of complexes that have been shown to decay via O−O bond homolysis, but is essentially identical to that for the decay of $[(TMC)Fe^{III}(OOH)]^{2+}$ in the presence of $HClO_4$, which has been proposed to undergo O−O bond heterolysis on the basis of the acid concentration dependence observed for its decay.[22b] Interestingly, a similar 10 kJ/mol enthalpy difference was found for the decay of acylperoxoiron(III) tetramesitylporphin intermediates by homolytic and heterolytic pathways.[23] In line with other observations reported here, the Eyring activation parameters obtained for the decay of **2** and rate of product formation support a mechanism involving rate-determining O−O bond heterolysis. This cleavage pathway would generate a short-lived $Fe^{V}(O)(OH)$ species (Scheme 1), which is proposed to be responsible for olefin oxidation.[4b] In fact, such a species has been detected for a related Fe(N4) complex by variable-temperature electrospray mass spectrometry.[11]

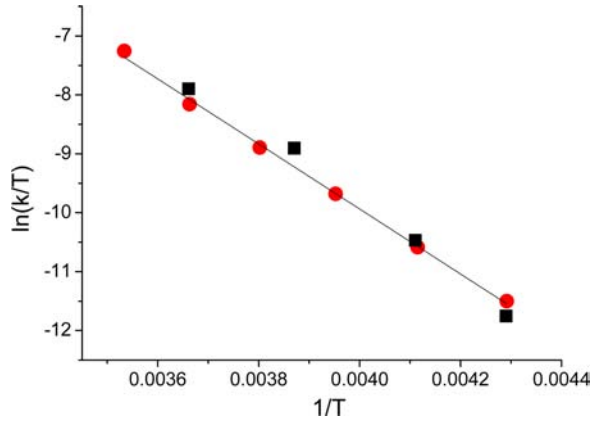

Figure 4. Eyring plot for the decay of **2** generated from 1.0 mM **1** and 10 equiv of 30% H_2O_2 in CH_3CN in the presence of 250 equiv of 1-octene (red circles) in the temperature range of −40 to 10 °C. Black squares represent k_{cat} values obtained from the rates of product formation.

Table 1. Eyring Activation Parameters for the Decay of (L)Fe^{III}-OOR Complexes

reaction	$\Delta H^{\ddagger}$, kJ/mol	$\Delta S^{\ddagger}$, J/K·mol	proposed O−O bond cleavage mode	ref
(TPA)Fe^{III}-OOH in CH_3CN	45(2)	−95(10)	heterolysis	*a*
(TMC)Fe^{III}-OOH + $HClO_4$ in CH_3CN	44(2)	−90(10)	heterolysis	22b
(TMC)Fe^{III}-OOH in acetone/CF_3CH_2OH	56(2)	−75(2)	homolysis	22c
(N4Py)Fe^{III}-OOH in acetone/CF_3CH_2OH	53(1)	−121(2)	homolysis	22c
(TPA)Fe^{III}-OO^{t}Bu in CH_3CN	52(1)	−74(3)	homolysis	22a
(TPA)Fe^{III}(κ^2-$O_2C(CH_3)_2OH$)	54(3)	−35(13)	homolysis	9b

[a]This work. Abbreviations: N4Py, *N*,*N*-bis(2-pyridylmethyl)bis-(2-pyridyl)methylamine; TMC, 1,4,8,11-tetramethylcyclam; TPA, tris(2-pyridylmethyl)amine.

In summary, we have shown that the (TPA)Fe^{III}-OOH complex **2** is the catalytically active species in olefin oxidation reactions catalyzed by Fe(TPA) and H_2O_2. The decay rate of **2**

dx.doi.org/10.1021/ja402759c | *J. Am. Chem. Soc.* 2013, 135, 6438−6441

matches that of product formation, indicating a rate-limiting step that involves decay of **2**. This decay rate accelerates as a function of water concentration and plateaus above 0.3 M, indicating a fast pre-equilibrium binding of water onto **2** followed by rate-determining decay of the water adduct. An H_2O/D_2O KIE of 2.5 is observed in the decay of **2** and in product formation, consistent with a proton-assisted O−O bond heterolysis of **2**, a notion also supported by the Eyring activation parameters. Taken together, these results provide the first kinetic evidence in support of the mechanism previously proposed for Fe(TPA)-catalyzed oxidations, involving rate-limiting formation of an $Fe^{V}(O)(OH)$ species from an Fe^{III}-OOH intermediate that is responsible for alkane and olefin oxidations, including those with high retention of stereochemistry (Scheme 1).[4b,5,9a] Given that several other iron catalysts supported by tetradentate nonheme ligands have been observed to exhibit oxidative reactivity similar to that of the $Fe(TPA)/H_2O_2$ system, the reaction sequence proposed in Scheme 1 is likely to serve as the mechanistic basis for this entire family of nonheme iron catalysts.[4b,9a,24]

■ ASSOCIATED CONTENT

Supporting Information

Table S1, decay rate of **2** as a function of olefin concentration; Figures S1−S4, UV−vis spectroscopic data for the accumulation and decay of **2** under various conditions, kinetic data for iron-catalyzed olefin oxidation under various conditions, and data fitting. This material is available free of charge via the Internet at http://pubs.acs.org.

■ AUTHOR INFORMATION

Corresponding Author

larryque@umn.edu

Notes

The authors declare no competing financial interest.

■ ACKNOWLEDGMENTS

This work was supported by the U.S. Department of Energy Office of Basic Energy Sciences (grant DE-FG02-03ER15455). We thank Prof. John D. Lipscomb for valuable discussions.

■ REFERENCES

(1) Sheldon, R.; Kochi, J. *Metal-Catalyzed Oxidations of Organic Compounds*; Academic Press: New York, 1981.

(2) (a) Tinberg, C. E.; Lippard, S. J. *Acc. Chem. Res.* **2011**, *44*, 280. (b) Costas, M.; Mehn, M. P.; Jensen, M. P.; Que, L., Jr. *Chem. Rev.* **2004**, *104*, 939. (c) Abu-Omar, M. M.; Loaiza, A.; Hontzeas, N. *Chem. Rev.* **2005**, *105*, 2227.

(3) (a) Que, L., Jr.; Tolman, W. B. *Nature* **2008**, *455*, 333. (b) Sun, C. L.; Li, B. J.; Shi, Z. J. *Chem. Rev.* **2011**, *111*, 1293. (c) White, M. C. *Science* **2012**, *335*, 807.

(4) (a) Chen, K.; Que, L., Jr. *Angew. Chem., Int. Ed.* **1999**, *38*, 2227. (b) Chen, K.; Costas, M.; Kim, J. H.; Tipton, A. K.; Que, L., Jr. *J. Am. Chem. Soc.* **2002**, *124*, 3026. (c) Ryu, J. Y.; Kim, J.; Costas, M.; Chen, K.; Nam, W.; Que, L., Jr. *Chem. Commun.* **2002**, 1288. (d) Oldenburg, P. D.; Feng, Y.; Pryjomska-Ray, I.; Ness, D.; Que, L., Jr. *J. Am. Chem. Soc.* **2010**, *132*, 17713.

(5) Feng, Y.; Ke, C. Y.; Xue, G. Q.; Que, L., Jr. *Chem. Commun.* **2009**, 50.

(6) (a) Wang, B.; Wang, S.; Xia, C.; Sun, W. *Chem.−Eur. J.* **2012**, *18*, 7313. (b) Wu, M.; Miao, C. X.; Wang, S. F.; Hu, X. X.; Xia, C. G.; Kuhn, F. E.; Sun, W. *Adv. Synth. Catal.* **2011**, *353*, 3014. (c) Lyakin, O. Y.; Ottenbacher, R. V.; Bryliakov, K. P.; Talsi, E. P. *ACS Catal.* **2012**, *2*, 1196.

(7) (a) Suzuki, K.; Oldenburg, P. D.; Que, L., Jr. *Angew. Chem., Int. Ed.* **2008**, *47*, 1887. (b) Costas, M.; Tipton, A. K.; Chen, K.; Jo, D. H.; Que, L., Jr. *J. Am. Chem. Soc.* **2001**, *123*, 6722.

(8) (a) Chen, M. S.; White, M. C. *Science* **2007**, *318*, 783. (b) Chen, M. S.; White, M. C. *Science* **2010**, *327*, 566. (c) Gomez, L.; Garcia-Bosch, I.; Company, A.; Benet-Buchholz, J.; Polo, A.; Sala, X.; Ribas, X.; Costas, M. *Angew. Chem., Int. Ed.* **2009**, *48*, 5720.

(9) (a) Chen, K.; Que, L., Jr. *J. Am. Chem. Soc.* **2001**, *123*, 6327. (b) Mairata i Payeras, A.; Ho, R. Y. N.; Fujita, M.; Que, L., Jr. *Chem.−Eur. J.* **2004**, *10*, 4944.

(10) Bassan, A.; Blomberg, M. R. A.; Siegbahn, P. E. M.; Que, L., Jr. *J. Am. Chem. Soc.* **2002**, *124*, 11056.

(11) Prat, I.; Mathieson, J. S.; Guell, M.; Ribas, X.; Luis, J. M.; Cronin, L.; Costas, M. *Nat. Chem.* **2011**, *3*, 788.

(12) In order to carry out the kinetic studies, the HOOH oxidant had to be added all at once. In previous work, HOOH was introduced via syringe pumping in order to maximize HOOH conversion into products and minimize side reactions such as HOOH decomposition. The conversion of HOOH decreased from 80% with syringe pumping vs 50% under the current reaction conditions, but the stereoretention observed in the oxidation products was identical to that obtained under the syringe pumping conditions.

(13) Kim, C.; Chen, K.; Kim, J. H.; Que, L., Jr. *J. Am. Chem. Soc.* **1997**, *119*, 5964.

(14) Makhlynets, O. V.; Rybak-Akimova, E. V. *Chem.−Eur. J.* **2010**, *16*, 13995.

(15) Thibon, A.; Jollet, V.; Ribal, C.; Senechal-David, K.; Billon, L.; Sorokin, A. B.; Banse, F. *Chem.−Eur. J.* **2012**, *18*, 2715.

(16) Park, M. J.; Lee, J.; Suh, Y.; Kim, J.; Nam, W. *J. Am. Chem. Soc.* **2006**, *128*, 2630.

(17) Unfortunately, these two adducts are not distinguishable by either UV−vis or EPR methods.

(18) Whittaker, J. W.; Lipscomb, J. D. *J. Biol. Chem.* **1984**, *259*, 4476.

(19) Dunford, H. B.; Hewson, W. D.; Steiner, H. *Can. J. Chem.* **1978**, *56*, 2844.

(20) (a) Traylor, T. G.; Xu, F. *J. Am. Chem. Soc.* **1990**, *112*, 178. (b) Groves, J. T.; Watanabe, Y. *J. Am. Chem. Soc.* **1988**, *110*, 8443.

(21) (a) Lee, S. Y.; Lipscomb, J. D. *Biochemistry.* **1999**, *38*, 4423. (b) Tinberg, C. E.; Lippard, S. J. *Biochemistry.* **2009**, *48*, 12145.

(22) (a) Kaizer, J.; Costas, M.; Que, L., Jr. *Angew. Chem., Int. Ed.* **2003**, *42*, 3671. (b) Li, F. F.; Meier, K. K.; Cranswick, M. A.; Chakrabarti, M.; Van Heuvelen, K. M.; Munck, E.; Que, L., Jr. *J. Am. Chem. Soc.* **2011**, *133*, 7256. (c) Liu, L. V.; Hong, S.; Cho, J.; Nam, W.; Solomon, E. I. *J. Am. Chem. Soc.* **2013**, *135*, 3286.

(23) Yamaguchi, K.; Watanabe, Y.; Morishima, I. *J. Am. Chem. Soc.* **1993**, *115*, 4058.

(24) Company, A.; Feng, Y.; Guell, M.; Ribas, X.; Luis, J. M.; Que, L., Jr.; Costas, M. *Chem.−Eur. J.* **2009**, *15*, 3359.